PRAMANA
— journal of
physics

Vol. 68, No. 2
February 2007
pp. 235–241

Optimization studies of photo-neutron production in high-Z metallic targets using high energy electron beam for ADS and transmutation

V C PETWAL[1], V K SENECHA[2], K V SUBBAIAH[3], H C SONI[1] and S KOTAIAH[2]

[1]Industrial and Medical Accelerator Section, Centre for Advanced Technology, Indore 452 013, India

[2]Power Supply Division, Centre for Advanced Technology, Indore 452 013, India

[3]Safety Research Institute, Indira Gandhi Centre for Atomic Research, Kalpakkam, India

E-mail: senecha@cat.ernet.in

Abstract. Monte Carlo calculations have been performed using MCNP code to study the optimization of photo-neutron yield for different electron beam energies impinging on Pb, W and Ta cylindrical targets of varying thickness. It is noticed that photo-neutron yield can be increased for electron beam energies ≥100 MeV for appropriate thickness of the target. It is also noticed that it can be maximized by further increasing the thickness of the target. Further, at higher electron beam energy heat gradient in the target decreases, which facilitates easier heat removal from the target. This can help in developing a photo-neutron source based on electron LINAC by choosing appropriate electron beam energy and target thickness to optimize the neutron flux for ADS, transmutation studies and as high energy neutron source etc. Photo-neutron yield for different targets, optimum target thickness and photo-neutron energy spectrum and heat deposition by electron beam for different incident energy is presented.

Keywords. Photo-neutrons; electron beam; metal targets; optimization; heat deposition; accelerator driven systems; transmutations.

PACS No. 29.25.Dz

1. Introduction

Facilities generating high intensity neutrons find applications in wide-ranging fields viz, boron neutron capture therapy (BNCT) for cancer treatment, nuclear, material science, condensed matter physics, polymer science, radioisotope productions, industries, biotechnology etc. In nuclear science and technology the measurements of neutron cross-sections for $(n, \gamma)(n, xn)$ and (n, f) reactions for the hybrid reactors and transmutation of long-lived isotopes are of immediate interest. Similarly, fusion reactor design technology needs important inputs for radiation damage of metals and alloys, tritium breading ratio and neutron multiplication, neutron spectrum and reaction rates in the blanket as well as structural shielding materials. Electron

LINAC-based neutron sources are inherently compact, economical, reliable, easy to handle, less hazardous in nature and most suitable for applications such as neutron capture and fission cross-section studies, radio-isotope production and basic neutron scattering experiments for material science studies.

Electron LINAC-based photoneutron sources have recently been used for the Reactor Accelerator Coupling Experiments (RACE) and for providing vital information about the coupling of sub-critical assembly with neutron source [1–3]. These sources are therefore proving themselves as an attractive alternative to spallation neutron sources. Although the process of conversion of electron beam via Bremsstrahlung and giant dipole resonance processes are not very efficient in neutron generation as compared to the spallation neutron process, however the reliability, low cost, compactness and ease of operation makes the electron-driven neutron source as a viable alternative. MCNP codes have been used for calculations of neutron yield through bremsstrahlung interactions of electron beam with low as well as high-Z metallic targets [4] for ADS application as well. Recently, photoneutron capabilities have been included in the code by introducing LAU150 library, which contains photonuclear cross-sections. The code has been used to simulate photoneutron generation from metallic targets bombarded by electron beams up to 150 MeV. In the first step, proper functioning of the code is checked by comparing the simulation results for a 1.68 cm thick lead target and the results published in IAEA 188 [5].

Applications of such neutron sources in ADS and transmutation require higher neutron yield along with less stringent heat deposition in the target assembly. MCNP simulations have been further extended to obtain the maximum photoneutron yield as a function of optimum target thickness and incident energy of the electron beam impinging on tantalum target. The neutron energy spectrum and the heat deposition rate in the target for various incident electron energies have been calculated. The photoneutron yield for 100 kW system with electron beam energy of 100 MeV can deliver a neutron yield of 2.34×10^{14} n/s (3.4×10^{14} at 150 MeV). Such a system can be used to drive a sub-critical assembly with k_{eff} value $\geq$0.95. Further the heat deposition rate which is critically dependent on the energy of the incident electron beam and target thickness suggest that one can work at higher incident energy getting higher neutron yield and producing less heat deposition density above 100 MeV energies.

2. Photoneutron production mechanism

When high-energy electrons impinge on a target material, continuous spectrum of bremsstrahlung photons is generated. These bremsstrahlung photons subsequently interact with the nucleus of the target material, resulting in the emission of the nucleons. This interaction is known as a photonuclear interaction. As the nucleons are bounded with the nucleus by binding energy (5–15 MeV), the photon should have energy above a threshold value to participate in the photonuclear reaction [6]. Photonuclear interaction is mainly the result of three specific processes: giant dipole resonance (GDR), quasi-deuteron (QD) production and intranuclear cascade. Between the threshold energy and up to $\sim$35 MeV, neutron production results

primarily from GDR. The physical mechanism can be described as one in which the electric field of the energetic photon transfer its energy to the nucleus by inducing an oscillation (known as giant resonance oscillation) which leads to relative displacement of tightly bound neutrons and protons inside the nucleus. Absorption of the incident photons excites the nucleus to a higher discrete energy state, and the extra energy is emitted in the form of neutrons. For heavy nuclei, the excited nucleus comes to the ground state by emission of neutron (γ, n). Some contribution from double neutron emission (γ, xn) is also possible for higher photon energies as shown by Kumar *et al* [4]. Because of the presence of the large Coulomb barrier, proton emission is strongly suppressed for heavy nuclei. The cross-section for this process has a maximum at photon energy between 13–18 MeV for heavy nuclei and 20–23 MeV for light nuclei ($A < 40$). The cross-section for giant resonance neutron production reduces rapidly, at photon energies >35 MeV, while at $50 < E < 140$ MeV, the photoneutron production is due to quasi-deuteron effect. In this process, the incident photon interacts with the dipole moment of a neutron–proton pair inside the nucleus rather than with the nucleus as a whole; hence the name quasi-deuteron. Above 140 MeV, photoneutrons are produced via photo-pion production.

3. MCNP code calculations

MCNP is a general purpose Monte Carlo code for solving radiation transport problems related to neutron, photon, electron and coupled neutron–photon or electron–photon in various mediums. Recently photonuclear physics for 12 isotopes has been introduced in MCNP by using LA150U photonuclear library with energies up to 150 MeV. The code treats an arbitrary three-dimensional configuration of materials in geometric cells bounded by first- and second-degree surfaces and some special fourth degree surfaces. As MCNP handles photon and neutron transport, it can further be used to simulate the cooling system and reflector, moderator etc to get neutrons of desired energy. F1 and F2 tally are used for flux and yield scoring. 10^6 histories are run to reduce statistical error less than 5%. Though neutron yield depends sensitively on the material and the geometry of the target, for comparison of the results and ascertaining the proper functioning of photonuclear physics included in the code, we have considered a lead target, for which measured results are available (cylindrical pallet with $r = 3$ cm and thickness 1.68 cm). Simulation results and measurement results are shown in figures 1 and 2.

3.1 *Photoneutron yield*

Photoneutron yield for tantalum target is calculated for different target thickness and for different electron beam energies.

$$\text{Neutron yield } \varphi_{\mathrm{n}} = N_0 \rho t \cdot \sigma_{\mathrm{T}}(E) \cdot \varphi_{\mathrm{e}}/M \ (\mathrm{n{\cdot}s^{-1}}),$$

where M, ρ and t are atomic mass, density and target thickness respectively. N_0 is the Avogadro number; φ_{e} the incident electron fluence rate (electron/s); $\sigma_{\mathrm{T}}(E)$ is the total photonuclear cross-section, where the sum of all the cross-sections of

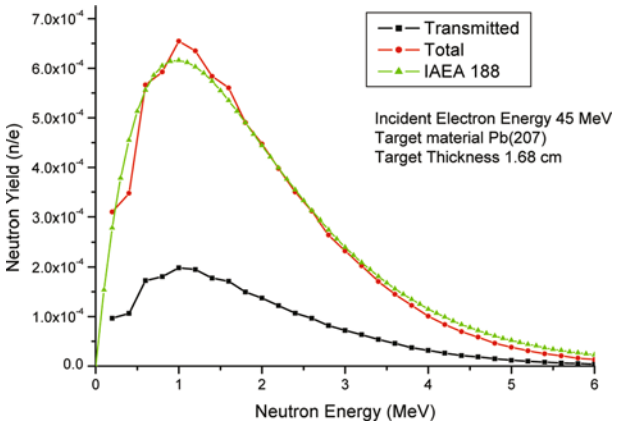

Figure 1. Comparison of neutron spectrum from lead target.

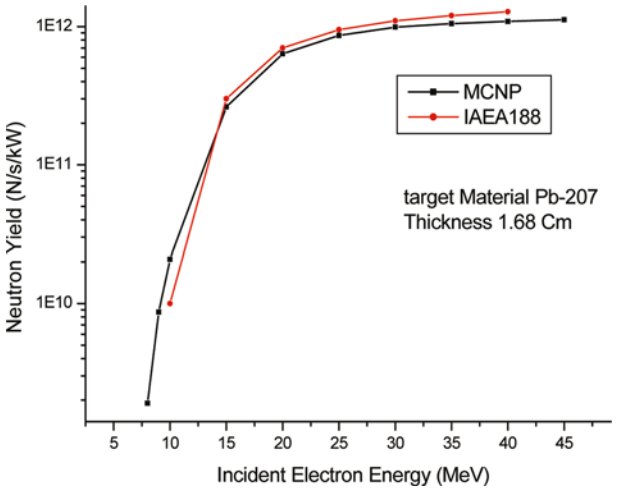

Figure 2. Comparison of the photoneutron yield from lead target.

processes is leading to neutron emission and E is the electron incident energy. Figure 3 shows neutron yield as a function of target thickness for various incident electron beam energies.

It is evident that maximum yield occurs at 5.6–6.0 cm thickness from the region where the slopes are greatest.

3.2 *Heat deposition in the target*

Figure 4 shows the heat deposition rate in the Ta target at 50, 100 and 150 MeV energies. It is noticed that the heat deposition at 100 MeV is nearly half of that in

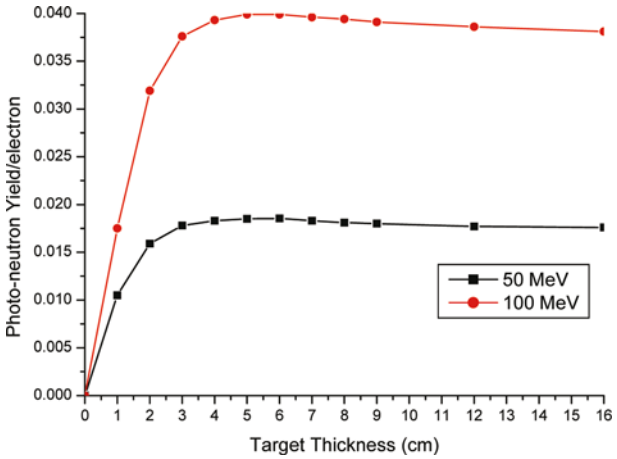

Figure 3. Photoneutron yield from Ta target as function of target thickness.

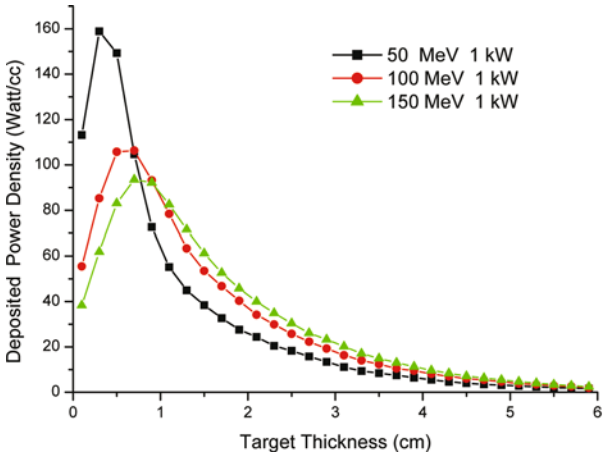

Figure 4. Heat deposition density as a function of target thickness for different incident electron energies (1 kW power).

the case of 50 MeV per kW of electron beam power. The FWHM and the peak value of heat deposition density for 50 MeV are 160 W/cc and 130 W/cc respectively.

This helps in efficient cooling of the target assembly which normally consists of targets in the form of disks of varying thickness with slight gap for cooling channels.

3.3 *Energy spectrum of photoneutrons*

The photoneutrons generated by 50, 100 and 150 MeV electron beams from a Ta-target are shown in figure 5. The spectrum can be well described by a Maxwellian distribution, which is dominated by the low energy neutrons with peak at ∼0.6 MeV.

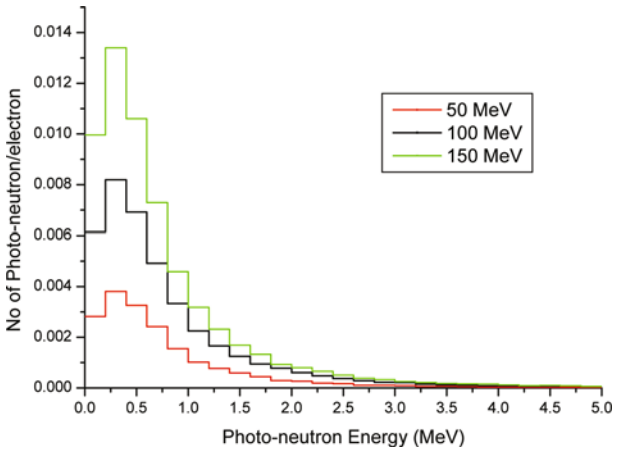

Figure 5. Photoneutron energy spectrum from Ta target.

The fitted equation of the distribution is

$$\frac{\mathrm{d}N}{\mathrm{d}E_n} = k \cdot \frac{E_n}{T^2} \mathrm{e}^{-E_n/T}.$$

Here T is a nuclear temperature (MeV), which is characteristic of a particular target nucleus and represents the most probable energy of the neutrons generated. T is found to be 0.57 MeV for Ta. Also from figure 5, it is clear that on increasing the target thickness the distribution of the neutrons does not change. Magnitude of the electrons in a particular energy band changes till the saturation thickness is achieved.

4. Conclusions

Photoneutron production from Ta, W and Pb targets have been studied for different electron beam energies and for different target thickness. The photo neutron yield was compared with the reported results published by IAEA reports and after this benchmarking exercise we extended it to higher electron beam energies. It is noticed that maximum neutron yield for Ta target is obtained at target thicknesses of 5.8 cm and 6 cm for 100 and 150 MeV respectively. The rate of heat deposition for 100 and 150 MeV energies for Ta target is nearly half of the value corresponding to 50 MeV energy case. Thus, the dual advantage of working with higher incident electron energy offers maximum neutron yield and less heat deposition rate in the target. The energy spectrum of neutron shows a peak at 0.6 MeV and a relatively smaller percentage of high energy neutrons (>10 MeV). The neutron yield for 100 kW electron beam at 100 MeV energies inducing photoneutrons in Ta target is 2.4×10^{14} n/s which can be coupled to a sub critical assembly with k_{eff} value above 0.95.

References

[1] Dennis Beller *et al*, *Proceedings of the 8th International Presentations to the Information Exchange Meeting on Actinide and Fission Product Partitioning and Transmutation*, OCED/NEA, November 2004 (Las Vegas, Nevada, 2004)

[2] Y Gohar *et al*, Acelerator Driven Subcritical Assembly; Concept Development and Analyses, *The RERTR-2004 International Meeting* (Vienna, Austria, Nov. 2004)

[3] MCNP – A General Monte Carlo N-Particle Transport Code, Version 4B, LANL, LA-12625-M, 1997

[4] V Kumar, H Kumawat, Uttam Goyal, A Polanski and P Sergey, Does the electron beam has prospects in ADSS? *DAE-BRNS Symp. on Nuclear Physics* held on December 26–30 (2002)

[5] W P Swanson, *Radiological safety aspects of the operation of electron linear accelerators*, IAEA T R, Technical Report Series No. 188, IAEA (1979)

[6] Measurement of Photoneutron Spectrum at Pohang Neutron Facility, G Kim *et al*, *Nucl. Instrum. Methods in Phys. Res.* **A485**, 458 (2002)